CHARACTERIZATION OF COLLAPSIBLE SOILS WITH COMBINED GEOPHYSICAL AND PENETRATION TESTING

Victor A. Rinaldi
Universidad Nacional de Cordoba, Cordoba, Argentina

J. Carlos Santamarina
Georgia Institute of Technology, Atlanta, USA

Emilio R. Redolfi
Universidad Nacional de Cordoba, Cordoba, Argentina

ABSTRACT: Loess is characterized by an open structure of fine volcanic sand and silt particles with connecting clay bridges and buttresses at contacts. At low moisture content, the formation presents high stiffness and shear strength. When the moisture content increases, the soil structure undergoes a sudden volume collapse. This experimental study of Argentinean loess includes laboratory tests (index properties, shear wave velocity, permittivity and conductivity) and field tests (CPT, SPT and down-hole seismic). Micro-level analytical models of electrical forces, suction and cementation are developed to gain insight into the observed behavior. It is shown that geophysical methods present significant advantages that are complementary to standard field measurements for the characterization of loess deposits.

1 INTRODUCTION

Loess is a windblown soil formation. The Argentinean loess is the largest deposit of its kind in the southern hemisphere. It is composed of minerals of volcanic origin and its thickness varies between 25 m to 60 m. It has low mass density and open fabric made of fine sand and silt particles connected by clay bridges (mostly montmorillonite and illite). In its undisturbed form, the Argentinean loess is a metastable-collapsible soil which undergoes sudden volume change when subjected to either wetting or loading.

The characterization of loess with low energy mechanical and electromagnetic parameters is a promising alternative on the basis of physical arguments. The methodology is equally promising from the applied engineering perspective: these parameters can be easily measured in situ with available technology. For example, transducers are readily included in penetration testing (electrical and seismic cone). In addition, non-invasive techniques can be used such as ground penetrating radar, electrical resistivity techniques, and seismic methods (reflection, refraction, surface waves, vertical seismic profiling). The interpretation of these boundary measurements can be enhanced with tomographic inversion to obtain the spatial distribution of measured parameters.

This paper presents the results of an extensive laboratory and field study of Argentinean loess, including shear wave velocity, complex permittivity and conductivity measurements on specimens at different moisture content, down-hole seismic test, standard penetration and static cone penetration testing. The effect of mean confining stresses and moisture content on collapse is addressed.

2 BACKGROUND - PRELIMINARY ANALYSES

2.1 Argentinean Loess

The most relevant properties of Argentinean loess and the differences with other similar deposits around the world are described in Teruggi (1957), Reginatto (1971), Reginatto and Ferrero (1973), Moll and Rocca (1991). A brief summary follows.

The mineralogy of Argentinean loess includes volcanic glass 50%, quartz 20-30%, plagioclase 10%, and clay minerals (illite and montmorillonite). Insoluble calcium carbonate nodules and microcrystals are found within the soil mass (often less than 8% - includes some $MgCO_3$); they formed during successive dry-wet cycles due to capillary ascension of bicarbonate followed by crystallization. Gypsum is frequently encountered in varying quantities

Calcium and sodium are the most common adsorbed ions; sodium is the most abundant cation in the pore fluid (saturation fluid was extracted from a loess-water slurry and ions were determined using flame photometry). The most common anions are sulfates and chlorides. The amount of soluble Na

and Ca salts varies between 0.4% and 1.2% by weight.

The grain size distribution consists of sand (5 to 15%), silt (40 to 60%), and clay-size particles (20 to 35%). The specific surface is controlled by the clay fraction and may range from 1 m^2/gr to more that 10 m^2/gr. A medium with such a broad grain size distribution is meant to have elaborate fabric and to present complex micro-scale phenomena.

The liquid limit ranges between LL=22-30, the plastic limit PL=16-20 and the plastic index PL=4-12. Both LL and PI increase with clay content. The coarse fraction has low coordination. The clay fraction forms connecting bridges between the coarser particles, and flocculated clay buttresses at the contacts between silt and sand particles (Figure 1). These clay structures and precipitated salts confer stability and cohesion to the soil.

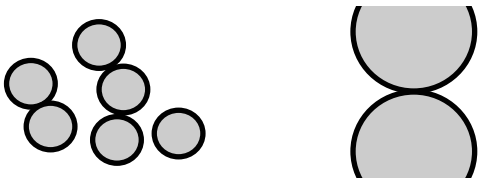

Figure 1: Clay in loess: bridges and buttresses.

Argentinean loess has low unit weight (γ_{dry}= 12.2 kN/m^3 to 13.7 kN/m^3). The specific gravity is Gs=2.65. The corresponding porosity ranges around n~0.5. The pore size distribution involves: submicron voids (5 to 25% - in terms of the volume of voids), 1-to-20 μm size voids (30 to 80%), and milimetric macro-porosity which is often internally coated with recrystalized carbonates. The closure of large pores upon collapse is documented in Lutenegger and Saber (1987).

The natural moisture content can range between 10% and 25%. Frequent values for unit weight in situ vary between γ_{moist}= 14 to 16 kN/m^3. The hydraulic conductivity is larger in the vertical direction than in the horizontal direction.

2.2 The Role of Moisture Content

Water plays a preponderant role in the formation and posterior behavior of loess. As the moisture content decreases, fine particles displace towards the menisci, the ionic concentration in the pore fluid increases, the thickness of double layers shrinks, and van der Waals attraction prevails over double layer repulsion. This evolution of interparticle electrical forces is captured in Figure 2. These results were computed with soil parameters applicable to clays in loess and platy particle geometry.

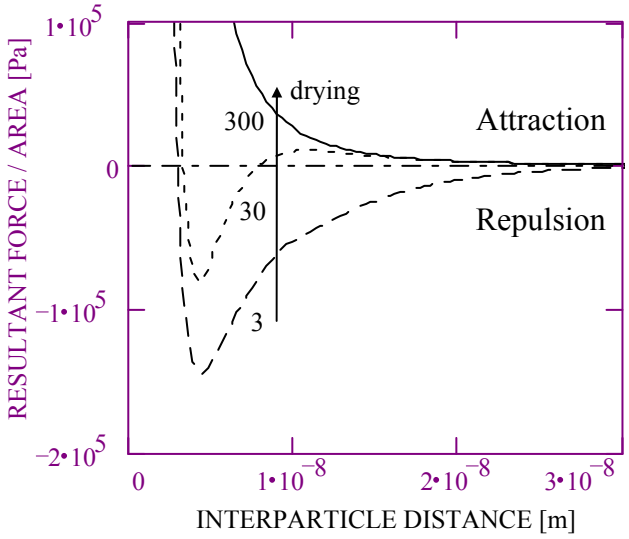

Figure 2. Increase in interparticle attraction as the moisture content decreases and the ionic concentration of the electrolyte increases (numbers indicate concentration in mole/m^3. Hydration and Born repulsion forces act at very small interparticle distance).

As the interparticle force-balance becomes attraction dominated, clay particles flocculate forming the clay bridges and buttresses at contacts sketched in Figure 1.

If the water content reduces even further, hydrated cations in the double layer dehydrate and ionically link two contiguous clay particles. In the meantime, the concentration of salts reaches saturation and salts precipitate as crystals that strengthen the soil structure.

Suction strengthens loess as well. Suction is more effective among platy clay particles in bridges and buttresses than at the meniscus between coarser spherical particles. This is clearly shown in Figure 3 (Note that the equivalent effective stress due to suction in spherical particles reaches a plateau and does not increase further).

The combined effect of these processes confers loess high cohesive strength which leads to surprising vertical cuts and the ability to withstand moderate loads.

Upon wetting, most of the processes that contribute to strengthening the soil mass are reversed:

- Soluble salt hydrates and softens
- The ionic concentration in the fluid continues decreasing with the increase in water content.

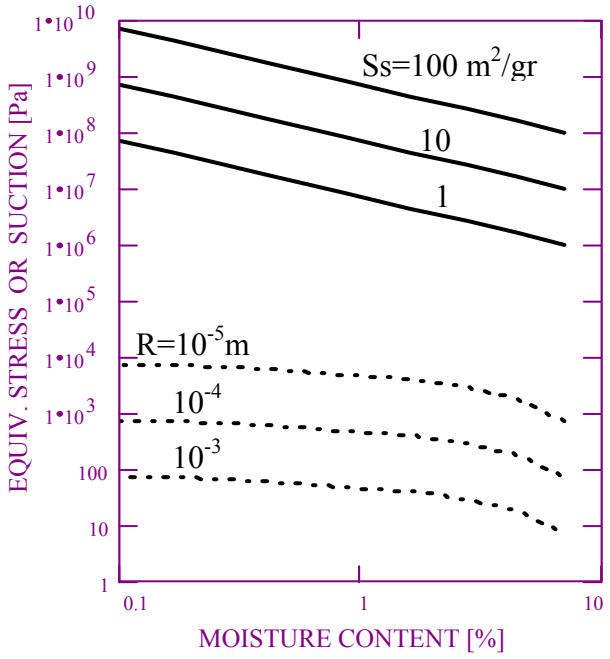

Figure 3. The effect of suction in granular media. Dotted lines correspond to spherical particles of radius R (equivalent compressive stress is shown). Continuous lines show the suction between parallel platy particles with different specific surface. No cavitation limit is presumed.

- The lower the ionic concentration the thicker the double layers that form around particles (this is aggravated by the low local confinement clay particles experience in clay bridges and buttresses). The shear stiffness and strength of the clayey formations decrease as the thickness of the hydration layers increases. Repulsion forces may become dominant and clay particles disperse.
- Suction gradually vanishes as saturation increases.

Eventually, the structure weakens and collapses even before full saturation is reached. Very low external loads are required to trigger the final collapse; in fact, self weight alone may suffice.

It is worth noting that a dry loess does not collapse when permeated with a non-polar fluid. This highlights the importance of clay and salt hydration in the metastable behavior of loess.

It follows from this discussion that strength, stiffness, and the extent of collapse will be affected by the initial void ratio and moisture content of the soil. Other relevant parameters include: fabric, the chemical composition of the saturating liquid, the amount of soluble salts, the amount of non-soluble cementing agents, the depth of burial or the level of external loads.

2.3 Cementation: Strength and Stiffness

The strength of cemented materials depends on the degree of cementation and the level of confinement. The higher the cementation and the lower the confinement, the stronger the role of cohesion on the peak strength. On the contrary, at sufficiently high confinement, the peak strength of particulate materials is friction dominated. The strength in the critical state is characterized by c=0 and ϕ independent of the degree of initial cementation.

Cementation has a significant effect on the stiffness of particulate materials, even for low degree of cementation. A modified Hertzian contact model was used to estimate the change in stiffness of the medium as a function of the cement content by weight of dry soil (Fernandez and Santamarina, 1998). Results presented in Figure 4 show the small-strain stiffness of the soil mass E_{soil} (normalized with respect to the shear modulus of the material of the particles, G_{mat}) vs. the effective confining pressure σ'_o (also normalized with respect to G_{mat}). These results show that even a very low cement content can have a very significant effect on the small-strain stiffness of the soil mass.

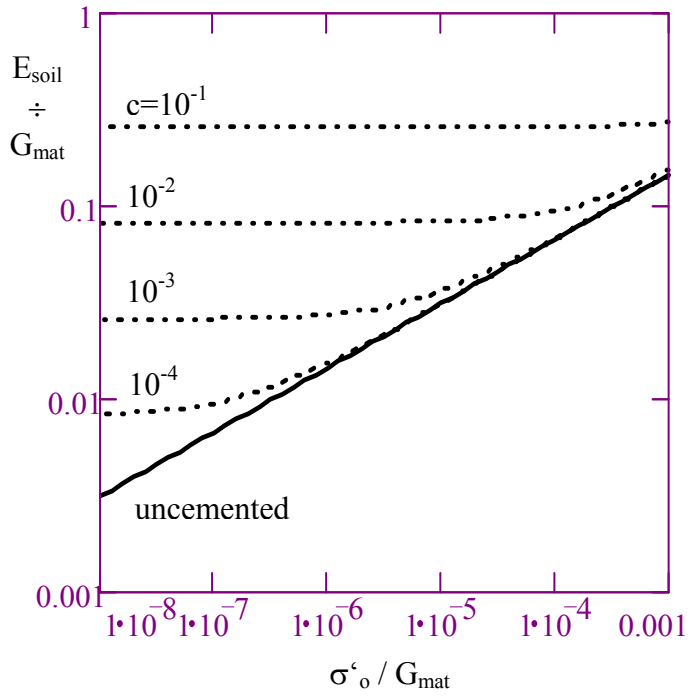

Figure 4. A small amount of cement has a very important effect on the small-strain stiffness of particulate materials (numbers indicate the cement content relative to the weight of dry soil).

2.4 Seismic Waves

Shear wave velocity V_s is related to the small-strain shear modulus G_{max} and the mass density of the medium ρ as

$$V_s = \sqrt{\frac{G_{max}}{\rho}} \quad (1)$$

In an uncemented particulate medium, Gmax depends on the state of effective stresses σ', as can be readily demonstrated with simple micromechanical models such as Hertzian contact in coarse particles or Coulombian forces in fine particles (see for example Cascante and Santamarina, 1996). Cementation at particle contacts reduces the sensitivity of the soil mass to the applied stresses, as shown above (Figure 4).

It follows from this discussion that the soil parameters that affect shear wave velocity are: void ratio e, effective confining pressure σ', degree of cementation, grain size distribution, soil structure and average coordination number. Empirical relationships for uncemented soils are power relations of the form:

$$G_{max} = A \cdot f_e \cdot \sigma'_o{}^{\alpha} \quad (2)$$

where A and α are constants and f_e is a function of the void ratio (Table 1 - see Ishihara, 1993)

Table 1: Typical parameter for Equation 2 corresponding to clayey soils (σ_o and G_{max} in kPa)

Soil Type	A	f_e	α	Reference
Stiff clays, Low PI 1.5>e>0.6	3270	$\frac{(2.97-e)^2}{1+e}$	0.5	Hardin & Black
Montmoril 2.5>e>1.5,	445	$\frac{(4.4-e)^2}{1+e}$	0.5	Marcuson & Wahls
Compres. Clays	90	$\frac{(7.32-e)^2}{1+e}$	0.6	Kokusho et al.

When G_{max} predicted in Equation 2 is introduced in Equation 1, a power relation between velocity and stress is predicted,

$$V_s = \varsigma \cdot \sigma'_o{}^{\alpha/2} \quad (3)$$

The sensitivity of shear wave velocity and penetration testing to the state of stress in soils allows for crude correlations between V_s and the number of blows N or the tip resistance q_c. The expressions are of the form:

$$V_s = \kappa \cdot N^{\delta} \quad (4)$$

$$V_s = \upsilon \cdot q_c{}^{\theta} \quad (5)$$

where κ, δ, υ and θ are constants. The values of the exponents δ and θ documented in the literature vary between 0.34 and 0.39 (Sykora and Koester, 1988; Olsen, 1988; Mayne and Rix, 1993). The main advantage of these correlations is to associate geophysical parameters to the extensive engineering design experience with penetration testing. However, these relations must be used with caution: the physical mechanisms involved in penetration testing (large-strain process) and in wave propagation (small-strain phenomenon) are very different. This is particularly relevant to cemented materials.

2.5 Electromagnetic Properties

The characterization of soils with electromagnetic techniques has significant advantages in the case of loess. There are three main parameters. The magnetic permeability μ is assumed very low due to low ferromagnetism (Note: there are iron salts in Argentinean loess - this confers loess the characteristic reddish-brown color). The permittivity ε of the medium is a measure of the polarizability of the medium. If it is determined in the high MHz region, the real permittivity correlates with the amount of free water in the soil. Finally, the conductivity of the soil is a measure of ion availability and ionic mobility; the amount of soluble salts, moisture content and fabric affect the electrical conductivity.

3 EXPERIMENTAL STUDY

The testing program involved a site south of the city of Cordoba. Both laboratory and field tests were conducted. The soil profile encountered at the site is characteristic of this formation:

0m to ~7m: low density silty clay - loess;
7m to ~11m: dense silty clay with cemented inclusions;
11m to ~13m: clean coarse sand and gravel; water table;
13.0 to end: stiff dense silty clay.

The values of Atterberg limits within the first

11m are fairly constant (LL = 25, PL = 20 and PI = 5). The battery of laboratory tests included index properties, shear wave velocity under isotropic confinement, conductivity and permittivity measurements.

Field tests involved down-hole seismic, SPT and CPT. These tests were repeated at the same site in three different locations

3.1 Shear Wave Velocity - Isotropic Cell

Isotropic tests were performed in a triaxial cell modified with bender elements. Specimens were trimmed from an undisturbed block sample recovered at a depth of 1.5 m. Two specimens were tested. One was air-dry (w= 3%). The other specimen was saturated while confined at 30 kPa (w= 25%). Backpressure was not used, yet full saturation is not required to reduce soil suction to very low values.

Confinement was increased in stages. For each load increment, the deformation of the specimen was monitored with a vertical LVDT, and measurements of wave velocity were repeated until constant values were obtained. Figure 5 shows the results.

The velocity is much lower for the saturated specimen than for the air-dry specimen, at the same confinement, and more sensitive to changes in confinement (particularly at higher confining pressure

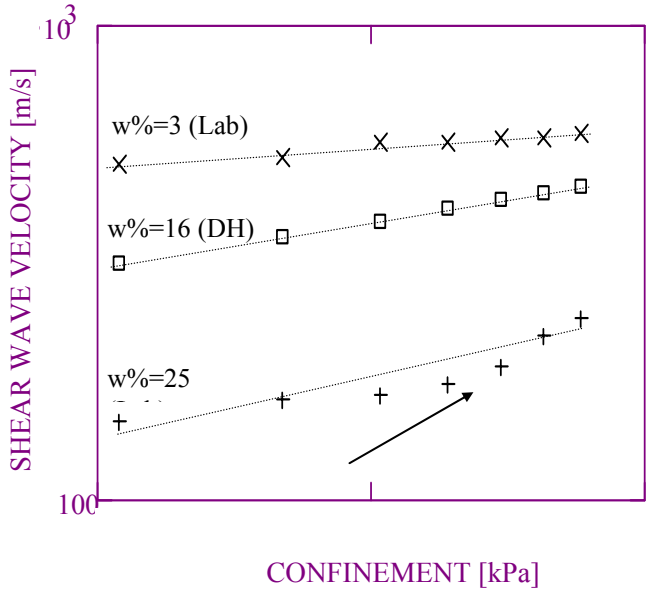

Figure 5. Shear wave velocity. (+) Laboratory measurements on undisturbed loess subjected to isotropic confinement; air-dry and saturated. (□) Down-hole seismic test in the field.

3.2 Shear Wave Velocity from Down-Hole Test

Signals were produced at the surface by striking a buried concrete block with a seismic hammer. The velocity for each stratum is obtained from the average slope of the travel time vs. depth plot at each depth. This approach reduces the amplification of high frequency noise in the data onto the inverted values of velocity (see Ballard 1976; Woods, 1978). Figure 5 shows the measured wave velocities as a function of the estimated mean confining stress σ_o, on the same plot with laboratory data.

3.3 Changes in Wave Velocity During Collapse

Small-strain V_P and V_S velocities were measured in a loess specimen during water infiltration to gain further insight into the behavior of loess during collapse. The test started with the specimen at its natural moisture content; the applied isotropic load was 50 kPa. Results are shown in Figure 6.

Collapse takes place within few minutes. The shear wave velocity decreases from V_S=256 m/s to 152 m/s. The longitudinal wave velocity decreases from V_P=405 m/s to V_P=260 m/s; this indicates that the material is not saturated even after collapse (V_P=1550 m/s for water). The sample continues deforming after collapse, yet, wave velocities remain constant.

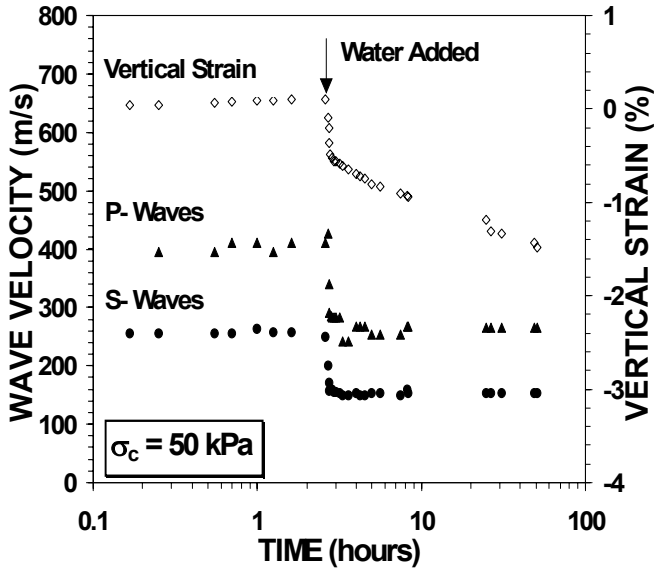

Figure 6. Loess collapse due to water infiltration. Undisturbed loess specimen subjected to constant confining pressure σ_o=50 kPa.

3.4 Penetration Resistance

SPT and CPT data are plotted in Figure 7

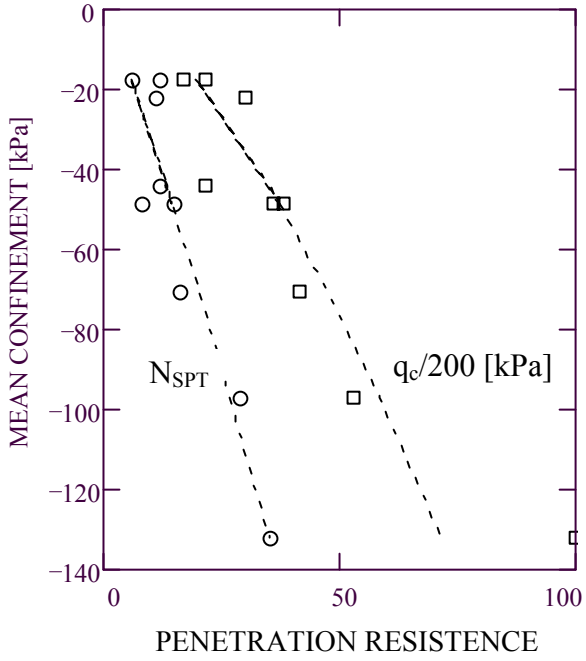

Figure 7. Penetration resistance vs. depth (in terms of mean confinement)

3.5 Conductivity

The electrical conductivity of undisturbed soil samples at different moisture content was determined with the two-electrode cell configuration. Figure 8 shows the results. The in situ electrical resistivity at different depths can be measured from the surface with the four electrode configuration or during penetration testing with electrodes mounted on the cone.

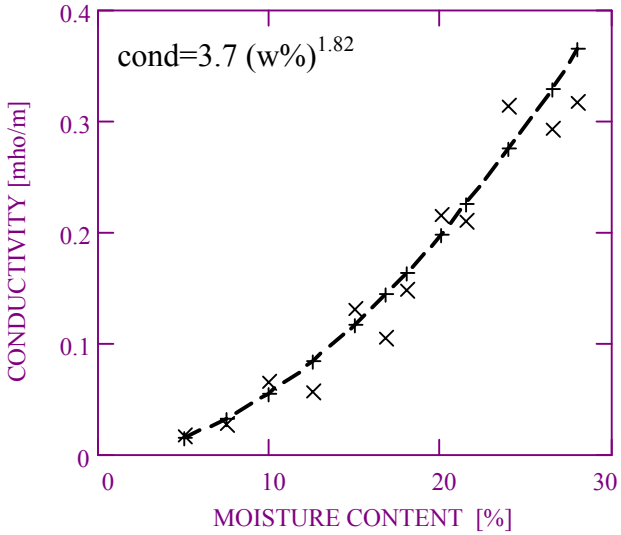

Figure 8. Variation of conductivity with moisture content (undisturbed specimens).

3.6 Permittivity

Undisturbed samples were trimmed into cylindrical specimens and moistened by capillarity by placing them on a porous stone in contact with deionized water for different periods of time. Moist specimens were kept in hermetic containers for homogenization. The complex permittivity was determined with a coaxial termination probe operating between 20 MHz and 1.3 GHz. After testing, the moisture content was determined. The real permittivity at 1 GHz is plotted vs. moisture content in Figure 9. The high frequency complex permittivity can be measured in situ with ground penetrating radar GPR, time domain reflectometry TDR, and during penetration testing with probes similar to the one used in this study.

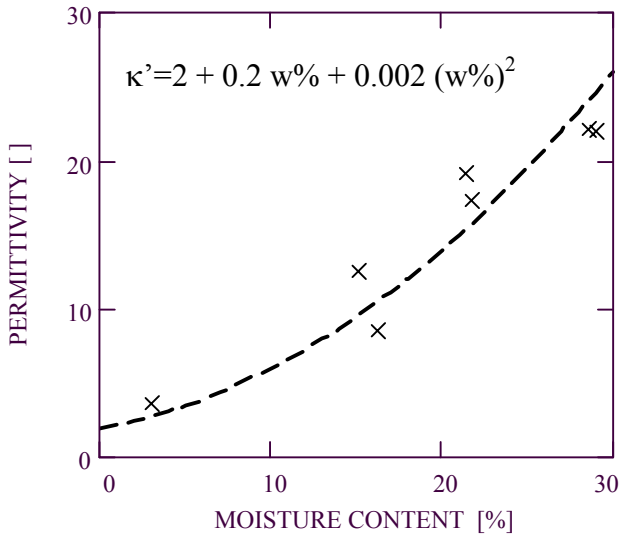

Figure 9. Permittivity vs. moisture content (1 GHz).

4 ANALYSIS AND DISCUSSION

4.1 Wave Velocity

The least squares fitting of the velocity-stress power relation to the data gathered in the laboratory renders the following fitting coefficients:

Lab air-dry	$V_s=370\cdot\sigma_0^{0.09}$
Lab saturated	$V_s=60\cdot\sigma_0^{0.24}$

where Vs is in m/s and σ_0 in kPa. On the other hand, the fitting of the power relation to down-hole measurements gives the following velocity-overburden relation:

Down-hole	$V_s=160\cdot\sigma_0^{0.19}$

For comparison, the expressions in Table 1 are evaluated for a void ratio e = 0.96:

Hardin & Black	$V_s=65\cdot\sigma_0^{0.25}$
Marcuson & Wahls	$V_s=41\cdot\sigma_0^{0.25}$
Kokusho et al.	$V_s=34\cdot\sigma_0^{0.3}$

Clearly, loess at natural moisture content has a significantly higher stiffness than standard clayey

soils, within the stress-range of these tests.

The exponent in velocity-stress relations reflects the combined effect of the geometry of contacts (e.g., spherical Hertzian $\alpha/2=1/6$; conical $\alpha/2=1/4$), changes in fabric (as density increases, the coordination number increases, and the exponent increases), and other physical processes at contacts (e.g., the yielding of spherical contacts leads to an exponent $\alpha/2=1/4$; deformation at contact governed by electrical interparticle forces manifests in high exponents, usually $\alpha/2>0.3$).

The low exponent for the air-dry specimen tested in the laboratory indicates that contact deformation and fabric changes are very limited. These results are in agreement with analytical predictions presented in Figure 4 for cemented particulate materials.

The higher exponent observed in the saturated specimen is consistent with values obtained for typical uncemented silts. Careful observation of the experimental results obtained for the saturated specimen (Figure 5 - w%=25 Lab) shows an upwards trend for the higher confinement, similar to the trends predicted in Figure 4. This suggests a change in behavior away from cementation controlled, towards a behavior controlled by contact deformation and fabric changes.

The estimation of effective interparticle forces is quite complex in soil systems with broad particle and pore size distribution. For example, clay particles in bridges and buttresses do not feel the direct impact of changes in external confinement. On the other hand, they directly experience suction and electrical forces which can be very high at low moisture (much higher than the effect of changes in external forces). Hence, changes in confinement and moisture content have different local effects within the soils mass.

Velocity trends obtained in the laboratory and in the field are superimposed in Figure 5. This graph accentuates the role of confining pressure and moisture content on the small-strain stiffness of loess. It is apparent that clay/salt bridges and buttresses creep with increased moisture, and the coarser particles effectively feel the overburden. This analysis also explains the weaker strength of loess with increased moisture content. It is important to realize that the creep of supporting bridges does not necessarily lead to the structural collapse of the soil skeleton: only virtual forces are required to prevent the buckling of grain-chains.

4.2 Wave Velocity and Penetration Resistance

The shear wave velocity obtained with down-hole testing was correlated with the penetration resistance corresponding to the same stratum. The fitting parameters are

SPT $V_s=180\cdot N^{0.23}$

CPT $V_s=370\cdot q_c^{0.28}$

where q_c is in kN/m^2 and V_s en m/s. These exponents are smaller in loess than in clays (0.35 to 0.7). The variability in these correlations discourages the use of small-strain parameters to estimate large-strain parameters, and vice-versa.

4.3 Electrical properties

The conductivity of loess is a function of the concentration and the mobility of ions. These depend on the availability of soluble salts and moisture content (soil structure and specific surface are also relevant - Rinaldi, 1994).

On the other hand, the high frequency polarizability of the medium assessed by the permittivity at 1 GHz is a measure of the free water content independent of soil characteristics and soluble salts (part of the water in the soil will be adsorbed and not free to rotate and align to the applied external field, hence it will not contribute to the measured polarization - Santamarina and Fam, 1997).

It follows from these observations that both permittivity κ' and conductivity provide complementary information relevant to the characterization of loess

5 CONCLUSIONS

Gravimetric forces prevail among sand and silt grains in loess. However, surface related electrical forces and suction prevail in clay particles. This distinction causes local segregation, and the formation of clay bridges and buttresses. The resulting material resembles a gap-graded, dual porosity medium, with unique and intricate behavior.

The cementation provided by precipitated salts, clay bridges and buttresses vanishes as the moisture content increases: suction forces disappear, precipitated salt crystals solubilize, the electrolyte concentration decreases and clay particles form thick double layers. The strength and stiffness of clay bridges and buttresses decrease, and the metastable soil structure provided by the coarse particles collapses. External forces increase the magnitude of the collapse.

Small-strain wave propagation velocity and large-strain strength depend on the applied confinement and moisture content. The lower the moisture

content, the less important the effect of confinement becomes. The reverse is also true.

The high frequency permittivity and the electrical conductivity of loess are robust indicators of moisture content, ionic concentration and ionic mobility.

ACKNOWLEDGMENTS

Support for this research was provided by national funding agencies CONICET (Argentina) and NSF (USA). D. Fratta made thoughtful comments and suggestions.

ELECTRONIC FILES & COMMUNICATION

Mathcad files used to compute Figures 2, 3, and 4 can be obtained from the authors. These files include assumptions, derivations, and numerical study. The authors can be electronically reached at:

vrinaldi@gtwing.efn.uncor.edu,
carlos@ce.gatech.edu,
eredolfi@com.uncor.edu.

REFERENCES

Ballard, R.F. 1976. Methods of Cross-Hole Seismic Testing. *ASCE Journal of Geotechnical Eng. Div*. 102:1261- 1273.

Cascante, G. & J.C. Santamarina 1996. Interparticle Contact Behavior and Wave Propagation. *ASCE Geotechnical Journal.* 122:831-839.

Fernandez, A. & J.C. Santamarina 1998. Cementation and Low strain Parameters. Submitted for Publication.

Ishihara, K. 1993. "Dynamic Properties of Soils and Gravels from Laboratory Tests", Soil Dynamics and Geotechnical Earthquake Engineering, Seco Pinto (ed.), Balkema, Rotterdam. pp. 1-17.

Lutenegger A.J. & R.T. Saber 1987. Pore Structure in Loess Using Mercury Porosimetry. *Engineering Aspects of Soil Erosion, Dispersive Clays and Loess*. Eds. C. W. Lowell & R. L. Wiltshire. ASCE. GSP10:115-128.

Mayne, P. W. & G. J. Rix, 1993. G_{max}-q_c Relations for Clays. *ASTM Geotechnical Testing Journal*. 16:54-60.

Moll, L. & R. Rocca 1991. Properties of Loess in the Center of Argentina. *IX Panamerican Conference on Soil Mechanics and Foundation Engineering*. Chile. Vol. 1.

Olsen R.S. 1988. Using the CPT for Dynamic Response Characterization. *Recent Advances In Ground Motion Evaluation*. ASCE SP20:374-388.

Reginatto, A.R. 1971. Standard Penetration Test in Collapsible Soils. *Fourth Panamerican Conference on Soil Mechanics and Foundation Engineering*. Puerto Rico. 77-84.

Reginatto A. R. & J.C. Ferrero 1973. Collapse potential of Soils and Soil Water Chemistry. *Proc. VIII International conference on Soil Mechanics and Foundation Engineering*. Moscow.

Rinaldi, V.A. 1994. Propiedades Dielectricas de los Loess del Centro de Argentina. *Tesis doctoral presentada en la Facultad de CEFyN.* Universidad Nacional de Cordoba. Argentina.

Santamarina, J.C. & M. Fam 1997. Dielectric Permittivity of Soils Mixed with Organic and Inorganic Fluids (0.02 GHz to 1.30 GHz). *J. Environmental & Engineering Geophysics,* 2:37-52.

Sykora, D.W. & P.J. Koester 1988. Correlation between Dynamic Shear Resistance and Standard Penetration Resistance in Soils. *Recent Advances In Ground Motion Evaluation*. ASCE SP20:389-404.

Teruggi M.E. 1957. The Nature and Origin of Argentinean Loess. *J. of Sed. Petrol*. 27:323-332.

Woods, R.D. 1978. Mesurement of Dynamics Soil Properties. *Earthquake Eng. and Soil Dynamics*, Pasadena. ASCE SP:91-121.